Ibn Al-Haitham Journal for Pure and Applied Sciences
Journal homepage: jih.uobaghdad.edu.iq
PISSN: 1609-4042, EISSN: 2521-3407
IHJPAS. 2026; 39(2)

Oxidizing Gas Sensing Using SnO_2 Thin Film Prepared by Thermal Evaporation Method

Zinah Abdulateef Abbas[1,2]*, and Seham Hassan Salman[2]
[1]Al-Nahrain Research Center for Renewable Energy, AL-Nahrain University, Baghdad, Iraq
[2]Department of physics, College of Education for Pure Science / Ibn Al-Haitham, University of Baghdad, Baghdad, Iraq
*Corresponding Author

Received: 6/September/2025
Accepted: 8/February/2026
Published: 20/April/2026
doi.org/10.30526/39.2.4294

Abstract

A SnOx thin film with a thickness of 400 ± 20 nm was deposited on a glass substrate and thermally oxidized at temperatures ranging from 573 K to 673 K. The structural surface morphology of SnOx thin films is checked. X-ray diffraction analysis indicated that films oxidized at 573K and 623K contain SnO, Sn3O4, and SnO2, as well as residual metallic tin. When the oxidation temperature was increased to 673K, the SnO_2 peaks became more prominent while the metallic Sn peak weakened. AFM studies indicated that the roughness of the films changed with different oxidation temperatures, which means that the oxidation temperature has a direct effect on the surface nature of the SnOx films. On the other hand, films oxidized at 673K (SnO2) are useful in gas sensor applications. The sensitivity (S) of the sensors manufactured for Oxidizing Gas (NO_2) was measured at room temperature and 373 and 473 K. The maximum sensitivity appeared for the sample at a 373 K operating temperature, which is 7.33%. The sample exhibited the lowest response time at an operating temperature of 473 K.

Keywords: SnOx, Thin films, X-ray diffraction (XRD), Surface roughness, Gas sensor.

1.Introduction

The sensing properties of tin oxide depend on changes in its lattice parameters. Therefore, it is an interesting semiconductor, and the values of these parameters can vary as a result of the combination of different tin oxide phases or due to the addition or subtraction of elements, usually while preparing [1]. These variations occur in the lattice structure. Constants are usually altered by semiconductor surface defects, and depending on the nature of the intrinsic defects, whether deep or surface, they produce variations in the semiconductor's optical properties [2]. Sn3O4 and SnO are two important unstable phases of tin oxide that can be obtained by controlling the pressure and temperature of oxygen. SnO is a p-type semiconductor; it has two transitions: direct (around 2.8 electron –Volt) [3].

The search for sensors capable of detecting nitrogen dioxide concentrations is critical. Nitrogen dioxide (NO_2), a common component of vehicle exhaust, is a major air pollutant. It is a toxic gas with a pungent odor, which not only pollutes the environment but also directly affects human health [4].

Metal oxide semiconductor oxygen sensors are a valuable research area due to their advantages of easy integration, good stability, long lifetime, low cost, small size, portability, and ease of operation [5].Various techniques have been used to synthesize tin oxides, such as hydrothermal [6], electron beam evaporation, DC sputtering, PLD, thermal chemical spraying, RF-sputtering. Sol-gel[7-14].

This paper focuses on how metallic Sn can be converted to SnOx thin films by oxygen flow and heat treatment on glass substrates and studies their structural, morphology and gas sensor performance.

2.Material and Methods

Tin oxide films were produced through a two‑step process. In the first step, pure metallic tin was thermally evaporated under a vacuum of about 3×10^{-2} mTorr, with the substrate positioned 18 cm above the molybdenum boat. A thin layer of approximately 400∓20 nm thickness was deposited, as determined by the molecular weight and optical method. In the second step, these films were oxidized by annealing at 573 °K, 623 °K or 673 °K for one hour.Tin oxide films were obtained in three phases. So SnO_x ,it mean (SnO,Sn_3O_4 and SnO_2).

Structural characterization was carried out using X‑ray diffraction (XRD 6000, Shimadzu, Japan), while surface morphology was examined via atomic force microscopy (AFM) using an SPM‑AA 3000 contact‑mode spectrometer (Angstrom, USA). Gas‑sensing performance was evaluated by monitoring the change in resistance over time as nitrogen dioxide was introduced at a fixed concentration and then switched off once saturation was reached. From these measurements, response and recovery times were determined for various operating temperatures, allowing the optimum operating temperature for maximum sensitivity to be identified. Sensitivity as a function of operating temperature was also assessed for samples oxidized at 673 °K.

3.Results

3.1. Structural Characterization

Figure 1 shows X-ray diffraction diagram and **Figure 1a** goes back to the tin where we notice the appearance of peaks (200), (101), (220), and (211) that agree with (ICDD No. 00-002-0709) and **Figure 5 b, c,** more information in **Table 1.**

Table1. Information obtained from XRD examination.

Temp. exidation°K)	cardNo.	phase	$2\Theta_{abs.}$	$2\Theta_{Astand.}$	D_{abs} (deg)	d_{astand}	hkl
Sn	00-002-0709	Sn-T	30.647	30.644	2.914	2.915	200
			43.902	43.871	2.060	2.062	220
			44.928	44.902	2.015	2.017	211
573	98-018-1280	SnO_2-O	30.847	30.909	2.896	2.891	121
		SnO_2-O	37.310	37.160	2.408	2.417	131
	00-020-1293	Sn_3O_4-A	18.527	18.315	4.785	4.840	100
623	98-018-1280	SnO_2-O	37.383	37.160	2.403	2.417	131
	00-020-1293	Sn_3O_4-A	18.573	18.315	4.773	4.840	100
	00-006-0395	SnO-T	30.110	29.868	2.965	2.989	101
673	98-018-1280	SnO_2-O	37.284	37.160	2.409	2.417	131
	00-020-1293	Sn_3O_4-A	18.494	18.315	4.793	4.840	100
	98-018-1280	SnO_2-O	44.059	44.314	2.053	2.042	221

Where: Sn-T(tetragonal Sn phase), SnO_2-O(orthorhombicSnO_2 phase), Sn_3O_4-A(Anorthic Sn_3O_4 phase), SnO-T(tetragonal SnO phase)

The crystallite size of thin films is calculated from **Equation 1**[15-16]

$$Cs = 0.94\,\lambda / \beta\cos\theta \quad \textbf{(1)}$$

The dislocation density δ, microstrain ε, and N_o were calculated through the following relationships: [17-20]

$$\delta = 1/Cs^2 \quad \textbf{(2)}$$

$$\varepsilon = \beta cos\theta/4 \quad \textbf{(3)}$$

$$N_o = t/(C.s)^3 \quad \textbf{(4)}$$

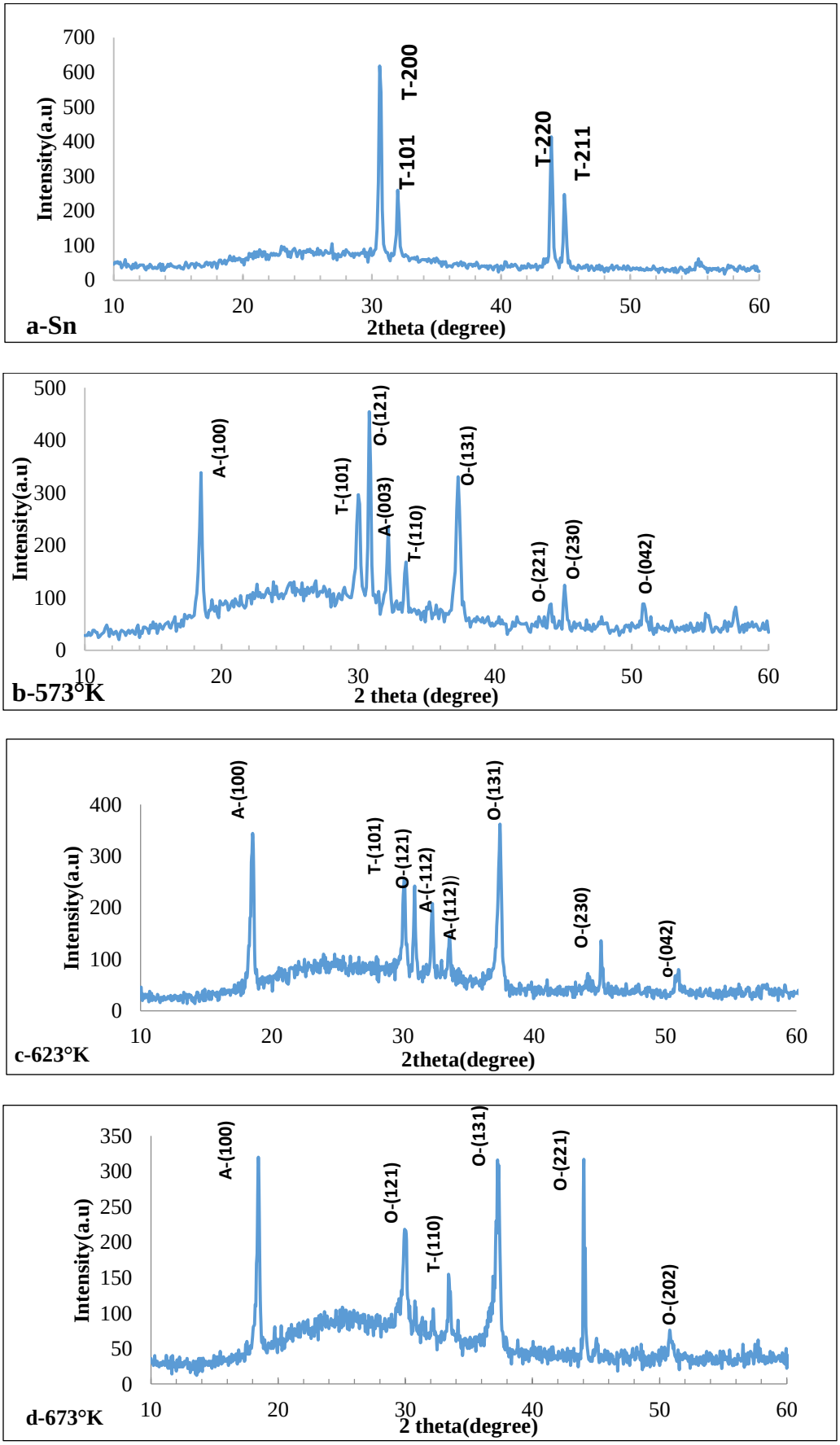

Figure 1. X-RD of Sn film oxidized at different temperature

3.2.Surface Morphology

Atomic force microscopy (AFM) was employed to examine the surface morphology. The results show that surface roughness varies with oxidation temperature, these changes are summarized in **Table 2.**

Table 2. Hkl, 2θ, phase, Cs, δ, ε and N_o

Temp K°	Hkl	$2\Theta_{abs.}$	Phase	β_{FHWM} deg	C.s nm	δ (line/m^2*10^{-3})	ε*10^{-3}	N_o
573	121	30.847	SnO2	0.2623	32.818	0.9284	1.1027	0.01131
623	131	37.384	SnO2	0.3043	28.79	1.2064	1.257	0.01676
673	131	37.285	SnO2	0.3564	24.691	1.6402	1.4656	0.0265

Table 3. AFM parameters.

Oxidation temp.(°K)	Mean diameter(nm)	Roughness(nm)	Root-mean-square (nm)
573	59.74	3.178	5.865
623	49.15	5.675	9.779
673	30.78	6.313	8.836

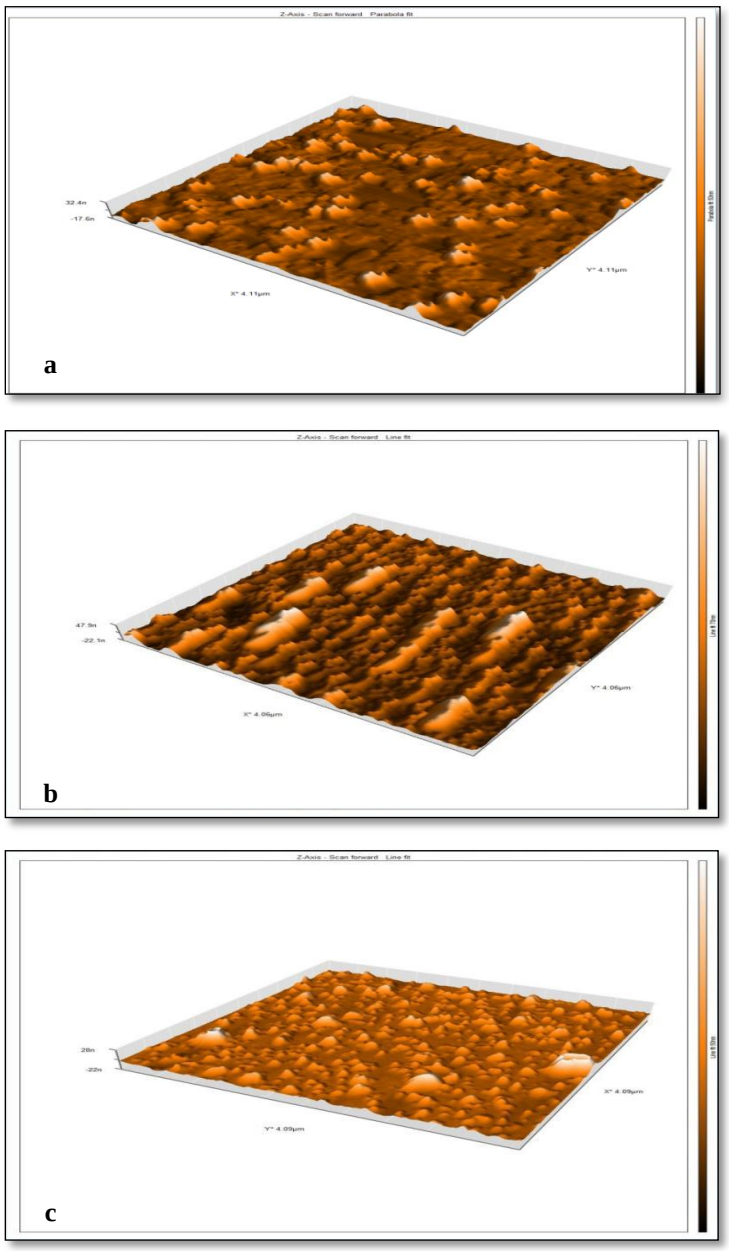

Figure 2.AFM images of samples at (a-573, b-623,c-673) °K.

3.3. The sensitivity results

The film oxidized at 673 °K was tested for sensitivity to NO_2 at a concentration of 20 ppm. **Figure 3** illustrates how the resistance of the SnO_2 membrane changes over time as nitrogen dioxide is introduced and then withdrawn.

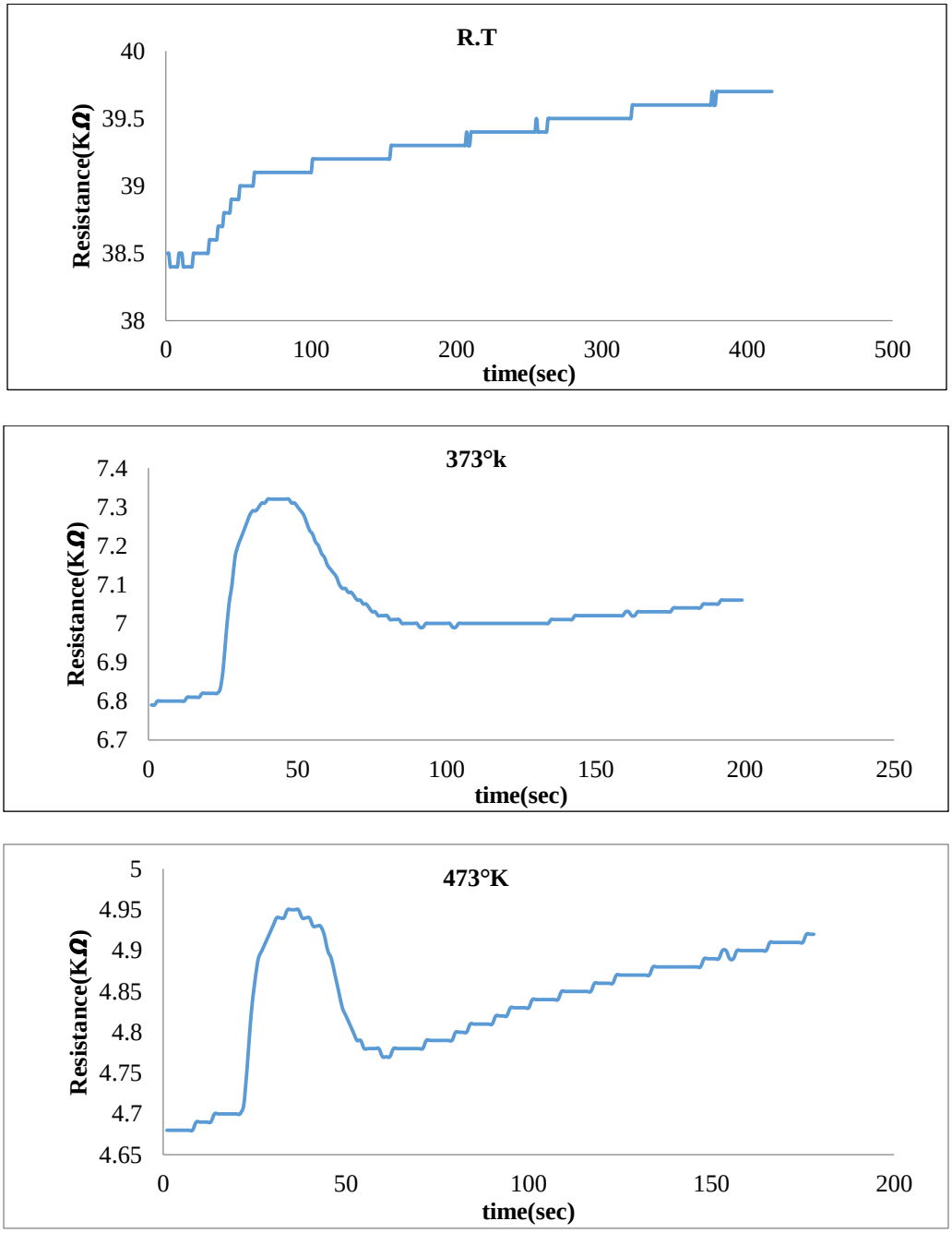

Figure 3. Change in the resistance of thin films exposed to NO_2 at various operating temperatures.

The sensitivity of the sensors can be found from the following relationship: [17, 21-24].

$$S=((Rg-R)/Rg) \times 100\% \quad \textbf{(5)}$$

Ra: resistance in air

Rg: resistance in the presence of gas.

The gas sensitivity was calculated using **Equation 5** for an oxidizing gas. **Figure 4** shows how the NO_2 gas sensitivity varies with the operating temperature.

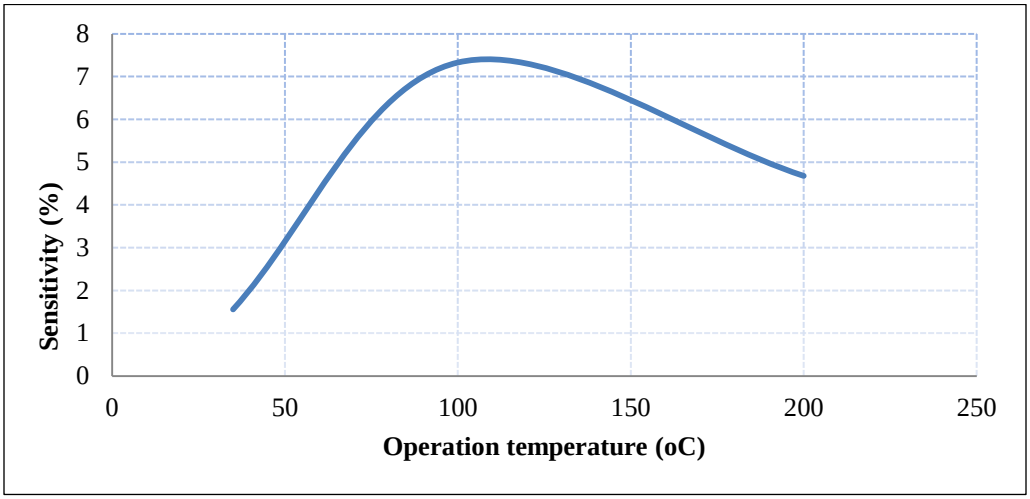

Figure 4. NO_2 gas sensitivity, versus operating temperature for thin films.

In **Figure 5,** the time required for the adsorption of gas molecules from the sample surface is long,

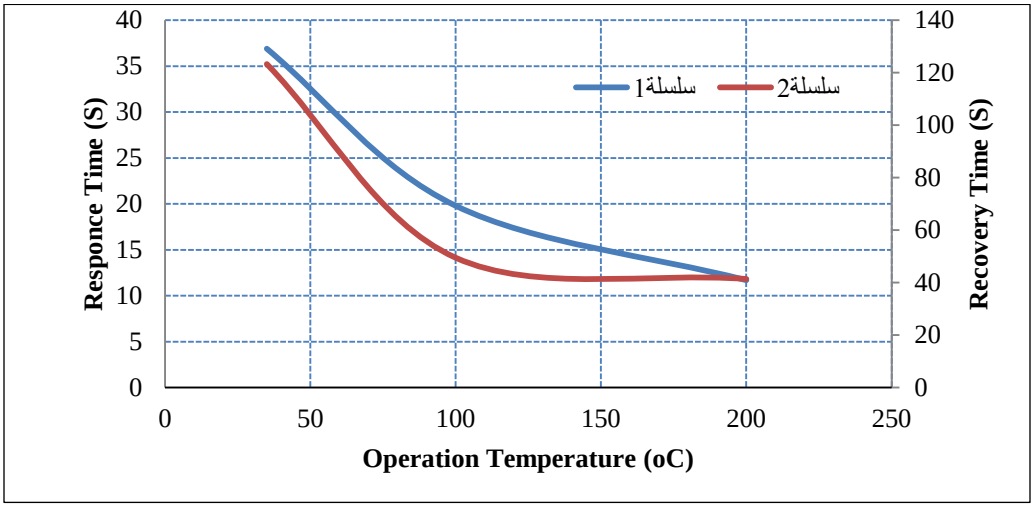

Figure 5. Response and recovery time versus operating temperature for SnOx film on glass substrates.

Table 4. S%, response and recovery time for thin films at (R.T,373,473) °K for gas (NO_2).

Operating Temp. (°**K**)	**Sensitivity (S%)**	**response time(sec)**	**recover time (sec)**
308	1.56	36.9	123.3
373	7.33	19.8	49.5
473	4.68	11.7	41.4

4.Discussion

X-ray diffraction analysis indicated that films oxidized at 573K and 623K contain SnO (JCPDS 00-001-0902), Sn_3O_4 (JCPDS 00-020-1293) and SnO_2 (JCPDS 98-018-1280) and residual metallic tin. When the oxidation temperature was increased to 673K, the SnO_2 peaks became more prominent; this indicates the dominance of that phase, while the metallic Sn peak weakened, indicating a higher degree of oxidation. These observations agree with the findings reported by Zarrinkhameh et al.[25,26]. Atomic force microscopy shows that roughness increace and grain size decreases with oxidation temperature. Films oxidized at 673K (SnO_2) exhibit greater surface roughness and smaller grain size, making them good candidates for gas-sensing applications. Upon exposure to Oxidizing Gas **(**nitrogen dioxide (NO_2)), the gas acts as an electron acceptor and withdraws electrons from the film surface. This decrease in free carriers leads to an increase in electrical resistance. Sensitivity is strongly influenced by nanoparticle size

because a high surface-to-volume ratio offers more active sites for gas adsorption[22]. So, the highest sensitivity of approximately 7.33 % was recorded at an operating temperature of 373K for (SnO_2) with a crystallite size of 24.69nm

So we found the recovery time to be higher than the response time. Also, it is noted that the lowest response time is at an operating temperature of 473 °C. Operating temperature, volumetric gas flow, and chamber size are factors on which response time and recovery time depend [27].

5.Conclusion

Tin oxide thin films with different temps. Oxidation has been successfully deposited after oxidation by the evaporation technique on glass substrates. The effect of oxidation temps. on properties was investigated. Films oxidized at 573K and 623K contain SnO, Sn_3O_4 and SnO_2 and residual metallic tin. When the oxidation temperature was increased to 673K, the SnO_2 peaks became more prominent; this indicates the dominance of that phase with a polycrystalline structure. We find that the less crystallite size of thin films is 24.69nm at oxidation temp. $673°K$. So, the highest sensitivity of approximately 7.33% was recorded at an operating temperature of 373K for (SnO_2). So we found the recovery time to be higher than the response time. Also, it is noted that the lowest response time is at an operating temperature of 473 K.

Acknowledgment

We gratefully acknowledge the support of the Thin Film Laboratory, Department of Physics.

Conflict of Interest

The authors declare that they have no conflicts of interest.

Funding

None.

References

1. Jayaprakash RN, Mariappan R. Effect of substrate temperature on the structural, optical and electrical properties of tin oxide thin films. Chalcogenide Lett. 2021;18(4):191–200. https://doi.org/10.15251/CL.2021
2. McCluskey MD, Janotti A. Defects in semiconductors. J Appl Phys. 2020;127:190401. https://doi.org/10.1063/5.0012677
3. Ling YL, Zhi ML, Hong TC, Zheng Y, Yuan YS, Ai HC. Phase and optical characterizations of annealed SnO thin films and their p-type TFT application. J Electrochem Soc. 2010;157(6):H598–H602. https://doi.org/10.1149/1.3385390
4. Comini E, Faglia G, Sberveglieri G. UV light activation of tin oxide thin films for NO_2 sensing at low temperatures. Sens Actuators B Chem. 2001;78(1–3):73–77. https://doi.org/10.1016/S0925-4005(01)00796-1
5. Dey A. Semiconductor metal oxide gas sensors: A review. Mater Sci Eng B. 2018;229:206–217. https://doi.org/10.1016/j.mseb.2017.12.036
6. Jiangyang LC, Wang QY, Yuan GXZ, Xishuang L, Peng SGL. Hydrothermal synthesis and gas sensing properties of flower-like Sn_3O_4. Sens Actuators B Chem. 2016;224:128–133. https://doi.org/10.1016/j.snb.2015.09.089
7. Wu G, Li F, Yu Z, Kong Z, Li YL, Zhi ML. Microstructure, optical and electrical properties of p-type SnO thin films. J Phys Conf Ser. 2021;1963:012003. https://doi.org/10.1088/1742-6596/1963/1/012003
8. Younus IA, Ezzat AM, Uonis MM. Preparation of ZnTe thin films using chemical bath deposition technique. Nanocomposites. 2020;6(4):165–172. https://doi.org/10.1080/20550324.2020.1865712
9. Shihui Y, Weifeng Z, Lingxia L, Dan X, Helei D, Yuxin J. Fabrication of p-type SnO_2 films via pulsed laser deposition using Sb dopant. Appl Surf Sci. 2013;286:417–420. https://doi.org/10.1016/j.apsusc.2013.09.107

10. Chalise R, Thakur PK, Nakarmi JJ, Shrestha SP. Preparation of SnO_2 thin films by spray pyrolysis and gas sensing application. J Nepal Phys Soc. 2021;7(2):144–150. https://doi.org/10.3126/jnphyssoc.v7i2.38635
11. Khalef WK, Hamza EK, Salman AA. Morphology, optical and electrical properties of SnO_2 thin films prepared by spray pyrolysis. Eng Tech J. 2015;33(3B). https://doi.org/10.30684/etj.33.3B.13
12. Hien VX, Lee JH, Kim JJ, Heo YW. Structure and NH_3 sensing properties of SnO thin films deposited by RF magnetron sputtering. Sens Actuators B Chem. 2014;194:134–141. https://doi.org/10.1016/j.snb.2013.12.086
13. Sun YL, Nabatame T, Chung JW, Sawada T, Miura H, Miyamoto M, Wenger C, Fischer I A. Compositional changes between metastable SnO and stable SnO_2 in sputtered films for p-type TFTs. Thin Solid Films. 2024;807:140548. https://doi.org/10.1016/j.tsf.2024.140548
14. Nwanna EC, Imoisili PE, Jen TC. Synthesis and characterization of SnO_2 thin films using metalorganic precursors. J King Saud Univ Sci. 2022;34:102123. https://doi.org/10.1016/j.jksus.2022.102123
15. Mustafa MH, Ali HM, Habubi NF, Hussein BH. Influence of annealing on optoelectronic properties of sprayed p-NiO/n-CdS. J Mater Sci Mater Electron. 2024;35(22). https://doi.org/10.1007/s10854-024-13259-z
16. Alsulami A, Alsalme A. Enhancement of structural, optical and optoelectrical properties of Sr-doped SnO_2 thin films. Physica B. 2025;699:416783. https://doi.org/10.1016/j.physb.2024.416783
17. Rodríguez-López J, Rangel R, Lara-Romero J, Quintana-Owen P, Bartolo-Pérez P, Ramos-Carrazco A. Structural parameters of ALD-SnO_2 thin films on Si substrates. J Ovonic Res. 2024;20(5):627–632. https://doi.org/10.15251/jor.2024.205.627
18. Verma A, Shriram K, Das B. Structural and optical characteristics of SnO_2 thin films grown at different substrate temperatures. J Optoelectron Biomed Mater. 2025;17(3):141–149. https://doi.org/10.15251/jobm.2025.173.141
19. Athab RH, Hussein BH. Fabrication and investigation of ZnTe thin films. Chalcogenide Lett. 2023;20(7):477–485. https://doi.org/10.15251/CL.2023.207.477
20. Khudayer IH, Hussein BH, Mustafa MH, Ibrahim AJ. Structural, optical and electrical properties of $AgInSe_2$ thin films. Ibn Al-Haitham J Pure Appl Sci. 2018;31(1). https://doi.org/10.30526/31.1.188
21. Hsieh JC, Liu CJ, Ju YH. Response characteristics of lead phthalocyanine gas sensor. Thin Solid Films. 1998;322:98–103. https://doi.org/10.1016/S0040-6090(97)00964-4
22. Kumar R, Mamta, Kumari R, Singh VN. SnO_2-based NO_2 gas sensor with outstanding sensing performance at room temperature. Micromachines. 2023;14(4):728. https://doi.org/10.3390/mi14040728
23. Najeeb JM, Mohammed Monawer E. Synthesis and characterization of NiO–CoO nanocomposite as CO_2 gas sensor. Samarra J Pure Appl Sci. 2025;7(2):170–184. https://doi.org/10.54153/sjpas.2025.v7i2.962
24. Hamdan AS, Ali IM. Enhancement of hydrothermal Co_3O_4 thin films as H_2S gas sensor by yttrium loading. Baghdad Sci J. 2019;16(1 Suppl). https://doi.org/10.21123/bsj.2019.16.1(suppl).0221
25. Zarrinkhameh M, Zendehnam A, Hosseini SM, Robatmili N, Arabzadegan M. Effect of oxidation and annealing temperature on SnO_2 properties. Bull Mater Sci. 2014;37(3):533–539. https://doi.org/10.1007/s12034-014-0702-1
26. Jamil SSB, Hateef AA, Atty HK. Physical properties of In_2O_3 thin films as CO_2 and H_2 gas sensors. Phys Sci Res Int. 2015;3(2):18–25. (no DOI available)
27. Chen W, Zhou Q, Wan F, Gao T. Gas sensing properties of nano-SnO_2 for hydrogen and carbon monoxide. J Nanomater. 2012;2012:612420. https://doi.org/10.1155/2012/612420